ELSEVIER

Neurobiology of Aging 29 (2008) 1256–1264

NEUROBIOLOGY OF AGING

www.elsevier.com/locate/neuaging

Age-related spatial learning impairment is unrelated to spinophilin immunoreactive spine number and protein levels in rat hippocampus

Michael E. Calhoun [a,b], Bonnie R. Fletcher [a], Stella Yi [a], Diana C. Zentko [a], Michela Gallagher [c], Peter R. Rapp [a,*]

[a] *Fishberg Department of Neuroscience, Kastor Neurobiology of Aging Laboratories, Mount Sinai School of Medicine, 1 Gustave L. Levy Place, New York, NY 10029-6574, United States*

[b] *Department of Cellular Neurology, Hertie Institute for Clinical Brain Research, University of Tübingen, Tübingen D-72076, Germany*

[c] *Department of Psychological and Brain Sciences, Johns Hopkins University, Baltimore, MD 21218, United States*

Received 22 September 2006; received in revised form 5 February 2007; accepted 7 February 2007

Available online 13 March 2007

Abstract

Age-related impairments in hippocampus-dependent learning and memory tasks are not associated with a loss of hippocampal neurons, but may be related to alterations in synaptic integrity. Here we used stereological techniques to estimate spine number in hippocampal subfields using immunostaining for the spine-associated protein, spinophilin, as a marker. Quantification of the immunoreactive profiles was performed using the optical disector/fractionator technique. Aging was associated with a modest increase in spine number in the molecular layer of the dentate gyrus and CA1 stratum lacunosum-moleculare. By comparison, spinophilin protein levels in the hippocampus, measured by Western blot analysis, failed to differ as a function of age. Neither the morphological nor the protein level data were correlated with spatial learning ability across individual aged rats. The results extend current evidence on synaptic integrity in the aged brain, indicating that a substantial loss of dendritic spines and spinophilin protein in the hippocampus are unlikely to contribute to age-related impairment in spatial learning.

Keywords: Hippocampus; Spinophilin; Rat; Aging; Morris water-maze; Learning; Memory; Stereology

1. Introduction

Aging in species from humans to rodents is frequently accompanied by mild cognitive impairment, including deficits in learning and memory revealed by tasks dependent on the hippocampus (reviewed in Gallagher and Rapp, 1997). There is significant variability among aged individuals, however, with some able to perform at a level equivalent to young adults, while others display relatively pronounced deficits. This pattern of cognitive aging has been most thoroughly characterized in rats, establishing a well-controlled animal model for studying the neurobiological basis of decline. Research adopting this approach has begun to yield a general consensus concerning the status of a wide range of neurobiological parameters that might contribute to cognitive decline during aging (reviewed in Bodles and Barger, 2004; Hof and Morrison, 2004; Rosenzweig and Barnes, 2003). The investigation reported here was prompted by a convergence of two such lines of inquiry. Growing evidence documents that neuron death in the hippocampus is not an obligatory consequence of aging or a necessary correlate of age-related cognitive decline (reviewed in Hof and Morrison, 2004). Related research in young adults indicates that dendritic spines in the mature brain retain a substantially greater capacity for morphological plasticity than previously presumed (reviewed in Halpain et al., 2005). Taken together, these emerging results have prompted considerable interest in the potential contribution to cognitive aging of changes in synaptic integrity. Relevant research has focused predominantly on presynaptic markers (Nicolle et al., 1999; Smith

* Corresponding author at: Fishberg Department of Neuroscience, Kastor Neurobiology of Aging Laboratories, Mount Sinai School of Medicine, Box 1065, 1 Gustave L. Levy Place, New York, NY 10029-6574, United States. Tel.: +1 212 659 5910; fax: +1 212 659 2510.

E-mail address: Peter.Rapp@mssm.edu (P.R. Rapp).

0197-4580/$ – see front matter © 2007 Elsevier Inc. All rights reserved.
doi:10.1016/j.neurobiolaging.2007.02.013

et al., 2000) and synaptic ultrastructure (Geinisman et al., 2004; Nicholson et al., 2004), however, and less is known about the influence of aging on the structure and function of dendritic spines, despite promising earlier research using Golgi labeling (reviewed in Coleman and Flood, 1987).

Spinophilin, a protein-phosphatase-1 (PP-1) binding protein that affects PP-1 activity, is thought to play a role in cytoskeletal scaffolding through actin binding (Allen et al., 1997; Brady et al., 2003; Satoh et al., 1998), and appears to be regulated by estrogen (Brake et al., 2001; Hao et al., 2003; Tang et al., 2004). Recent results also suggest a prominent role in synaptic plasticity, demonstrating that spinophilin is phosphorylated by ERK (Futter et al., 2005), and regulates both calcium signaling (Wang et al., 2005), and dendritic spine morphogenesis (Terry-Lorenzo et al., 2005). Although spinophilin protein levels vary regionally (Allen et al., 1997), it is detectable in the vast majority of dendritic spines (Ouimet et al., 2004), and several recent studies have confirmed the utility of this marker in quantitative light microscropic analyses (Hao et al., 2003; Radley et al., 2005; Tang et al., 2004). Here we investigated changes in the total number of spinophilin immunoreactive puncta and protein levels in the hippocampus of young and aged rats in relation to individual differences in spatial learning ability.

2. Methods

2.1. Subjects

Groups of mature adult (8 months) and aged (24–26 months), male Long-Evans rats were used for the morphological ($n = 8/16$ adult/aged) and protein level studies ($n = 13/28$ adult/aged) detailed below.

2.2. Behavioral testing

The cognitive testing procedures, performance measures and analytic strategy used in the current study have been validated extensively, as described elsewhere (Gallagher et al., 1993; Rapp and Gallagher, 1996; Smith et al., 2000). The primary outcome measure (i.e., spatial learning index) is a composite score of distance from the escape platform location during interpolated probe trials over the course of training in the water maze. This parameter provides a continuously distributed score of spatial learning ability that is relatively insensitive to the effects of aging on non-specific performance factors and that reveals considerable individual variability among aged subjects (Gallagher and Rapp, 1997).

Briefly, rats received eight consecutive days of behavioral testing in the spatial version of the water maze with three trials per day (60 s inter-trial interval, ITI). The escape platform remained in the same location during this phase of testing, submerged just under the surface of opaque water. Animals entered the maze at one of four points along the perimeter of the apparatus, with the start location varied across trials. Rats that failed to reach the platform within 90 s were gently guided to the escape location where they remained for 30 s. The last trial of every other session was a probe test in which the platform was retracted to the bottom of the maze for the first 30 s of the trial. Search patterns were recorded throughout training by a video-tracking system with custom-developed software (HVS Imaging, Hampton, UK). Standardized measures of spatial learning and memory, validated in many previous studies (reviewed in Gallagher et al., 2003), included: (1) cumulative search error, calculated from subjects' proximity to the escape platform during training trials, and (2) a spatial learning index, reflecting the degree of spatial bias for the escape location during the interpolated probe trials. Accurate search focused on the escape location results in low values for the latter measure. Rats subsequently were tested for one additional day on a cued version of the water-maze (six trials, 30 s ITI) with the raised, visible platform varied in location across trials.

2.3. Morphological studies

2.3.1. Tissue processing and immunostaining

Sacrifice and tissue-processing were as previously described (Smith et al., 2000). Briefly, approximately 2-weeks following behavioral testing, rats were deeply anesthetized with chloral hydrate, and perfused transcardially with a 1 min flush of ice-cold 1% paraformaldehyde in 0.1 M PBS, followed by 9–14 min of ice-cold 4% paraformaldehyde in PBS with 0.125% glutaraldehyde (65 ml/min). After perfusion, brains were removed and blocked in the coronal plane, post-fixed for 6 h, and stored at 4 °C in PBS with 0.1% sodium azide (PBS-az). Rats with evidence of pituitary tumors were excluded. Serial sections were cut on a vibratome (50 μm thickness, instrument setting) through the entire hippocampus, and stored at 4 °C in PBS-az until immunostaining.

Visualization of spinophilin-immunoreactive dendritic spines was accomplished using a novel staining approach involving a combination of techniques adapted from electron and light microscopy, as previously described (Hao et al., 2003; Tang et al., 2004). Briefly, sections were washed thoroughly in PBS, and pretreated with PBS/0.1% Triton-X (PBS-T) for 30 min at 4 °C. Sections were then incubated with a polyclonal rabbit antibody against spinophilin (1:200,000; courtesy of Drs. Patrick Allen and Paul Greengard) (Allen et al., 1997) in 3% normal goat serum (NGS) in PBS-T for 40 h at 4 °C. Sections were then washed in PBS and PBS-T before immunostaining with a goat anti-rabbit IgG antibody coupled to small (10 nm) gold particles (1:100; Electron Microscopy Sciences (EMS), Hatfield, PA) in 3% NGS in PBS-T for 2 h at room temperature. Sections were again washed in PBS before post-fixation in 2% glutaraldehyde in PBS. Following washes in distilled water, the immunostaining was enhanced using a silver-enhancement kit (Aurion R-Gent; EMS), using time of development (average approximately 30 min) to match staining across runs. Sections were washed again in distilled water followed by PBS, and were then mounted on slides, allowed

to air-dry, and cover-slipped using DPX mounting medium (EMS). All staining was performed blind, batches included an equal number of sections from each group, and the order of processing of sections was randomized. Because of the considerable interval (>2 years) between time of sacrifice and immunostaining, we performed a pilot study in a group of recently perfused rats and observed no qualitative differences in the pattern of immunostaining or puncta density.

2.3.2. Quantification of spine puncta

We have previously used stereological methods to quantify the total number of synaptophysin-positive pre-synaptic boutons at the light-microscopic level (Boncristiano et al., 2005; Calhoun et al., 1996, 1998), and the methods for spinophilin-positive spine number largely parallel those previous studies. Delineation of hippocampal subregions in this rat model has also been previously described (Rapp and Gallagher, 1996; Smith et al., 2000). The optical fractionator technique (West et al., 1991) was tailored to match the technical requirements for counting densely packed puncta such that the disector area (9 μm^2) was large enough to allow identification of individual puncta without obscuring them, and the depth (4 μm) optimized to clearly identify puncta as they came into focus, while permitting sufficient focal distance to minimize hardware variability in the *Z*-axis measurement. Post-processing section thickness was measured at each sampling site. Stereological sampling parameters for each of the regions are given in Table 1. For the molecular layer of the dentate gyrus, the location of each disector was recorded along a line perpendicular to the granule cell layer. Similar to our previous study (Smith et al., 2000), disectors within 25% of the total molecular layer thickness immediately adjacent to the granule cell layer were classified as residing in the inner molecular layer (IML; the target of intrinsic commissural/associational hippocampal connectivity), the adjacent 40% was considered the middle molecular layer (MML; the recipient of input from the medial entorhinal cortex), and the most distal 35% comprised the outer molecular layer (OML; the target of input from the lateral entorhinal cortex). Stereological sampling and counting was aided by StereoInvestigator software (MicroBrightField, Williston, VT), coupled to a Leica DMRB microscope, Ludl MAC-2000 *XYZ* stage controller and Optronics video camera. Regional borders were defined at 10×, and counting of immunoreactive puncta in optical disectors, as well as section-thickness measurements, were performed using a 100×, 1.4 NA oil-immersion objective.

Average puncta cross-sectional area was also measured at independent locations in the same sections. High-resolution images (1280 × 1024 pixels) were taken with a cooled digital camera (MagnaFire; Optronics, Goleta, CA) using the same microscope and 100× objective as in the analysis of puncta number. An average of 36 systematic-randomly placed locations through CA1 stratum radiatum from each rat were then analyzed using custom-designed measurement tools implemented with NIH-Image software (developed at the US National Institutes of Health and available on the Internet at http://rsb.info.nih.gov/nih-image/). Individual puncta (average 357/rat) were identified within a 2D optical disector frame and the area of each punctum was manually delineated.

2.4. Protein level studies

2.4.1. Sample preparation

Rats were deeply anesthetized by isoflurane inhalation, and in order to facilitate equally rapid brain removal across age groups, the skull was thinned along three grooves with a dental drill. Animals were then decapitated, and after removal, the brain was submerged in ice-cold Ringer's solution bubbled with 95% O_2. The hippocampus was then dissected from the surrounding tissue, laid flat, and 400 μm coronal slices through the rostral two-thirds of the structure were cut on a McIlwain tissue chopper. Three slices from each rat (approximately every fifth slice with a random start) were then washed in ice-cold PBS, frozen on dry-ice, and stored at −80 °C.

Samples were homogenized in 200 μl buffer (150 mM NaCl, 20 mM Tris, 0.1% SDS, 1% Triton-X 100, pH 8.0

Table 1
Numbers of counted puncta, section thickness, and sampling parameters for stereological analysis of spinophilin puncta number

Region	*XY* sampling (μm)	Average thickness (μm)	Number of disectors	# counted	Total number	N_v (#/μm^3)	V_{ref} (mm^3)
DG iml	350	12.6	24	115	4.90E + 07	0.13	0.42*
DG mml	350	12.6	38	185	7.80E + 07	0.14	0.67*
DG oml	350	12.6	28	136	5.64E + 07	0.13	0.59*
CA3 SLuc	120	13.9	71	304	1.63E + 07	0.12	0.15
CA3 SR	230	12.9	87	374	7.00E + 07	0.12	0.59
CA3 SLM	150	14.0	84	354	3.11E + 07	0.12	0.28
CA1 SR	350	11.0	91	473	1.75E + 08	0.15	1.24
CA1 SLM	250	12.6	78	315	6.92E + 07	0.11	0.65

As illustrated by the formula below, total number is computed by sampling a known fraction of the volume containing the entire region and multiplying by the reciprocal of the sampling parameters. The section sampling fraction (ssf) was one-tenth in all cases; the area sampling fraction (asf) is the ratio of disector area (9 μm^2) and the distance between disectors squared, which varied depending on the size of the region; and finally the thickness sampling fraction (tsf) is the ratio of the disector height (3 μm) to the measured section thickness. For reference, the numerical density (N_v) of puncta, and the region volume (V_{ref}) are also provided. Total number = (# counted) * ssf * asf * tsf = x * ssf * (*XY* sampling/disector area) * (average thickness/disector height) # = (# counted) * 10 * ((*XY* sampling^2)/9) * (average thickness/4). *: Computed as fraction of DG total (1.68 mm^3) based on sampled sites (see method text).

with 2× complete proteinase inhibitor cocktail (Roche, Indianapolis, IN), boiled for 5 min, homogenized, sonicated for 1 min, and frozen at −80 °C. Protein concentrations were measured using a Lowry-based detergent-compatible colorimetric assay (BioRad, Hercules, CA).

2.4.2. Western blots and quantification

For each gel, a standard curve of three concentrations was included. Laemmli sample buffer (Bio-Rad) was added to the samples before loading on the gel, and 15 μg of total protein was loaded in each lane. Samples were resolved by SDS-PAGE on 10% polyacrylimide gels before electroblotting onto Hybond ECL Nitrocellulose Membranes (Amersham, Piscataway, NJ). Membranes were blocked in 10% nonfat skim milk in PBS + 0.25% Tween-20 (PBST) for 1 h before incubation with anti-spinophilin (1:10,000; courtesy of Drs. Allen and Greengard, Rockefeller University) or anti-actin (1:1000; MAB1501R, Chemicon, Temucula, CA) in blocking buffer overnight at 4 °C. Membranes were then washed in PBST before incubation with the appropriate horseradish-peroxidase conjugated secondary antibodies (Vector Laboratories, Burlingame, CA) diluted 1:1000 in blocking buffer for 2 h at room temperature. Membranes were washed and immunoreactivity was visualized by ECL (Amersham) and exposure to film (Amersham). Films were scanned and mean optical density was analyzed with NIH Image. Each sample was run on two different gels with random loading orders, balanced between groups, and the average of the two optical densities was computed for each rat. As a control, results for spinophilin were compared to parallel immunoblots with actin. Although the actin quantification revealed no group differences (not shown), the values exhibited greater than expected variability, and thus uncorrected values for spinophilin are reported.

3. Results

3.1. Spatial memory

The outcome of behavioral testing was consistent with many previous investigations using the same study population (reviewed in Gallagher et al., 2003), and only a brief description is provided. As a group, aged rats displayed significant spatial learning deficits relative to young adults, as measured by both search error on the training trials (repeated measures ANOVA, main effect of age $F(1, 63) = 18.3$, $p < 0.0001$) and spatial learning index (Fig. 1; $F(1, 63) = 30.7$; $p < 0.0001$). There was considerable individual variability, however, and whereas a subset of aged rats exhibited impaired spatial searching during probe testing compared with young animals, other aged rats scored as accurately as young controls (Fig. 1). The distribution of this performance measure thereby provided a valuable background for evaluating the cognitive effects of aging in relation to the morphological and biochemical data. Rats in this study population did not show deficits

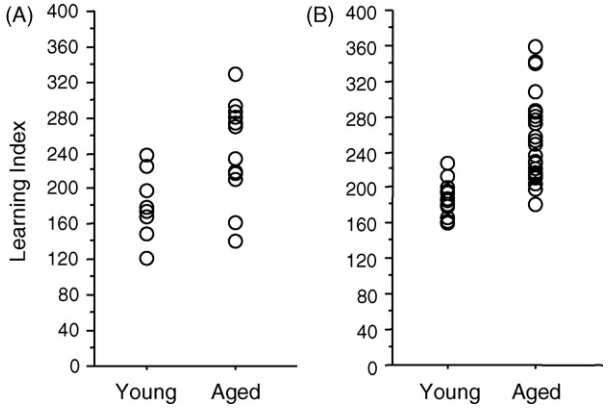

Fig. 1. Water maze learning index scores for individual young and aged rats included in the morphological (A) and biochemical (B) analyses (low values represent better performance). Note the presence of an overall age-related impairment, and the increased variability among the aged rats.

in the cued version of the water maze (path length; $F(1, 63) = 2.8$; $p > 0.05$), similar to previous reports (Gallagher and Rapp, 1997).

3.2. Spinophilin immunostaining

The general appearance of spinophilin immunoreactivity was similar to previous descriptions, with prominent labeling of the richly innervated synaptic zones of all hippocampal subfields (Fig. 2A), along with scattered cellular labeling. Staining intensity was relatively uniform across hippocampal subregions, but slightly higher in CA1 stratum radiatum, and both darker and more granular in CA3 stratum lucidum, with stratum lacunosum-moleculare of both CA1 and CA3 revealing the least intense immunostaining. Qualitatively, there were no differences with age or cognitive status.

At higher magnification, the punctate staining visualized by silver intensification of ultrasmall gold particles revealed a pattern of immunoreactivity consistent with labeling of individual dendritic spines. Numerous puncta were observed in all hippocampal subregions, ranging in diameter from 0.25–1.0 μm, and often organized in a linear arrangement, as would be expected for individual spines along a traversely sectioned dendrite (Fig. 2B–D). Control staining absent the primary antibody did not reveal granular puncta or any dark/patterned immunostaining other than occasional diffuse signal around blood vessels. Electron microscopic examination of post-embedding immunogold labeling in the hippocampus, revealed that the vast majority of dendritic spines were spinophilin-positive (Janssen, Morrison; personal communication).

3.3. Total number and size of immunoreactive spines

Stereological techniques were used to quantify the total number of immunoreactive puncta within optical disectors spaced throughout each of the hippocampal subregions (see

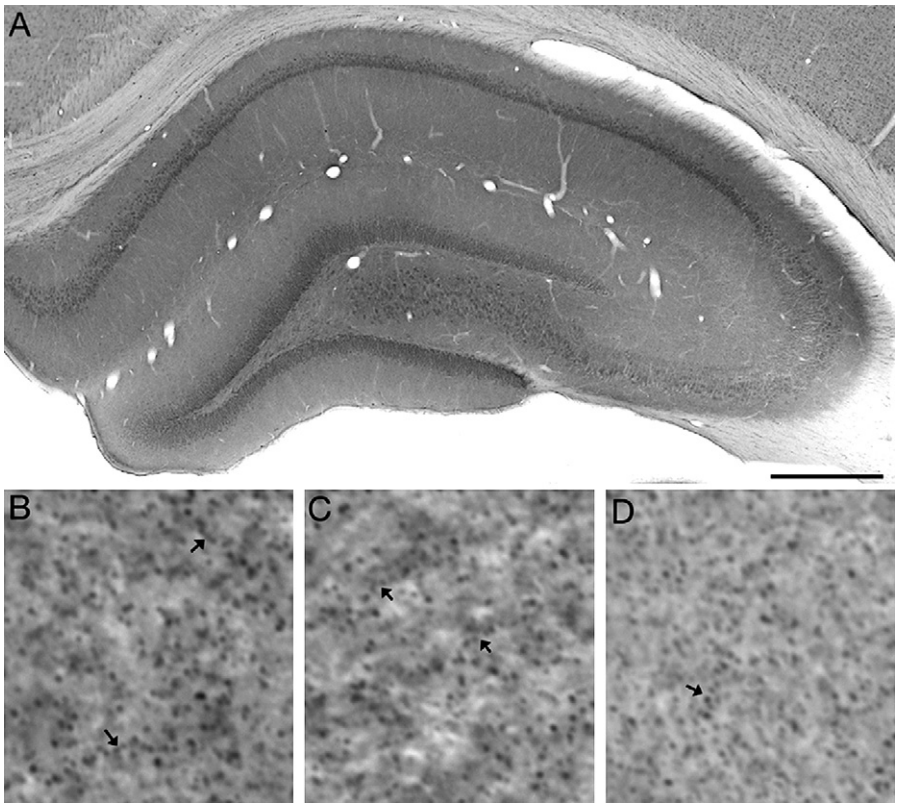

Fig. 2. Spinophilin immunoreactivity in the hippocampus. (A) Dense immunolabelling was apparent in all hippocampal subregions. Higher-magnification images from CA1 SR (B); CA1 SLM (C); DG (D) reveal the typical punctate pattern of immunostaining, with arrows indicating puncta arranged longitudinally. Scale bar: 500 μm in A, and 6 μm in B–D.

Table 1). Individual puncta could be readily resolved while focusing through the tissue despite their relatively small size, as the immunostaining provided high contrast and a 'crisp edge'.

The quantitative results failed to reveal a difference in spinophilin-immunoreactive puncta in relation to cognitive status in any region examined (comparisons between aged-impaired and aged-unimpaired for individual regions: $0.22 < p < 0.82$). Instead, the data demonstrated a modest increase in the number of spines with aging independent of cognitive status (Fig. 3; repeated measures ANOVA, main effect of age: $F(1, 22) = 5.2$; $p < 0.05$) in most, but not all hippocampal subregions (region × age interaction, $F(1, 7) = 3.9$; $p < 0.001$). Significant age-related differences were observed in DG IML ($F = 7.7$; $p < 0.05$) and OML ($F = 4.6$; $p < 0.05$), and CA1 SR ($F = 7.5$; $p < 0.05$). In no region was a correlation found in relation to spatial memory performance (example CA1 SR; Fig. 3B).

Because identification of individual immunolabelled spines is at the resolving limit of the light microscope, we were concerned that the reported effect of age might be related to a shift in spine size. In addition, it is possible that the age-related cognitive deficits are associated with a change in spine morphology or spinophilin protein content, in the absence of any overt change in spine number. Thus, we also estimated the average diameter of stained puncta in CA1 SR using stereological sampling and custom-designed analysis tools. As indicated in Fig. 4, no differences were observed with age ($F = 2.1$; $p = 0.16$) or cognitive status ($F = 1.02$; $p = 0.38$), and a histogram of individual puncta diameters revealed a very similar distribution across groups.

3.4. Spinophilin protein level

In order to test whether the morphological observations resulted from a change in protein level, and to independently confirm that there was no loss of spinophilin with aging, we also measured spinophilin protein content by Western blot (Fig. 5). Homogenates were made from hippocampal slices sampled from the anterior two-thirds of hippocampus. Immunoblots using spinophilin antibody revealed the expected 38 kDa band, and intensity was within the linear range for all individual rats according to the concentration standards run on each gel. Quantification of relative protein level did not indicate any difference with aging (Fig. 5B; $F(1, 39) = 0.21$), difference between the aged-impaired and aged-unimpaired ($p = 0.90$), or a correlation with cognitive status (Fig. 5C; $R^2 = 0.01$).

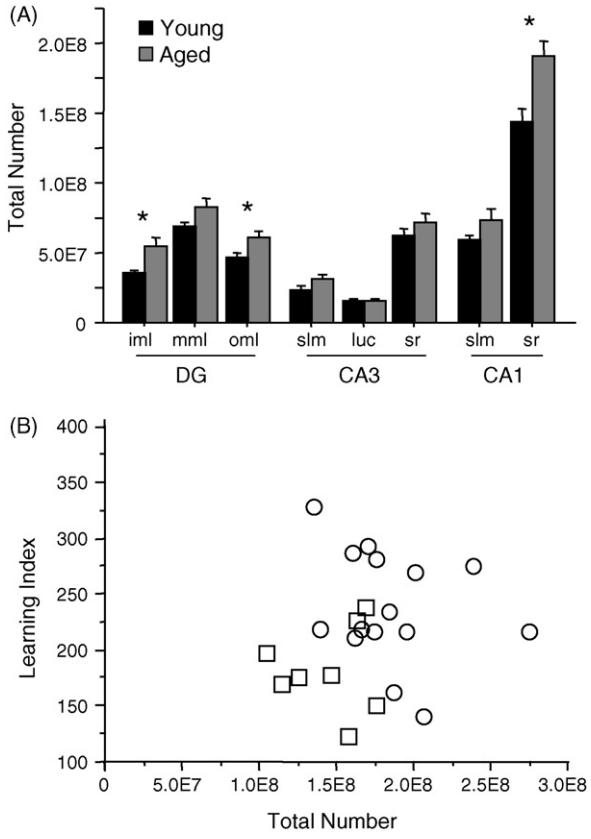

Fig. 3. Total number of spinophilin-positive spines (+S.E.M.). (A) The mean number increased with age in several subregions (* for comparisons with p values less than 0.05). (B) Scatterplot of CA1-sr spine number and learning index scores for individual subjects (squares: young; circles: aged). As in the other regions, no relationship was seen between these parameters.

4. Discussion

Spinophilin, a protein highly enriched in dendritic spines (Allen et al., 1997; Ouimet et al., 2004), has been strongly implicated in synaptic plasticity (Futter et al., 2005; Morishita et al., 2001; Terry-Lorenzo et al., 2005; Wang et al., 2005). The findings reported here demonstrate that normal cognitive aging is associated with an overall preservation of spinophilin protein content, together with no decline in immunoreactive puncta number or diameter in the rat hippocampus. These results add to a growing body of evidence that the structural integrity of the hippocampus is substantially less vulnerable to normal aging than previously thought (e.g., Geinisman et al., 2004; Rapp and Gallagher, 1996; Rasmussen et al., 1996), and that the basis of age-related cognitive decline is more likely to involve alterations in functional connectivity (e.g., Nicholson et al., 2004; Smith et al., 2000). It is interesting to note that in this study population, changes in presynaptic markers (Smith et al., 2000) can occur independent of changes in spinophilin. In this regard, the present results leave open a potential role for spinophilin in cognitive aging that might be selectively observed under conditions that engage the dynamic regulation of memory-related plasticity, including synaptic remodeling.

The quantitative approach adopted here is relatively novel, and given that immunoreactive labeling of dendritic spines approaches the resolving power of the light microscope, it is appropriate to consider whether the morphometric data are influenced by methodological factors. It is noteworthy in this context that the total number of synapses the CA1 field of the hippocampus, identified by electron microscopy in the same study population of young and aged rats (Geinisman et al., 2004), substantially exceeds the reported estimates of total spinophilin-positive puncta. These findings suggests that the approach we used underestimates dendritic spine number, perhaps as a consequence of limited resolution for distinguishing gold particle labeling associated with multiple, closely adjacent spines. Nonetheless, the same quantitative strategy has proved sufficiently sensitive to detect reliable effects of ovarian hormone manipulations on spinophilin-positive spine number in monkeys (Tang et al., 2004). In the present experiment, this approach also revealed reliable regional differences in spine number across the principal fields of the hippocampus (Fig. 3). Accordingly, while it would be inappropriate to view the data as a quantitatively accurate estimate of absolute spine number, they provide a sensitive, valid basis for examining relative differences in

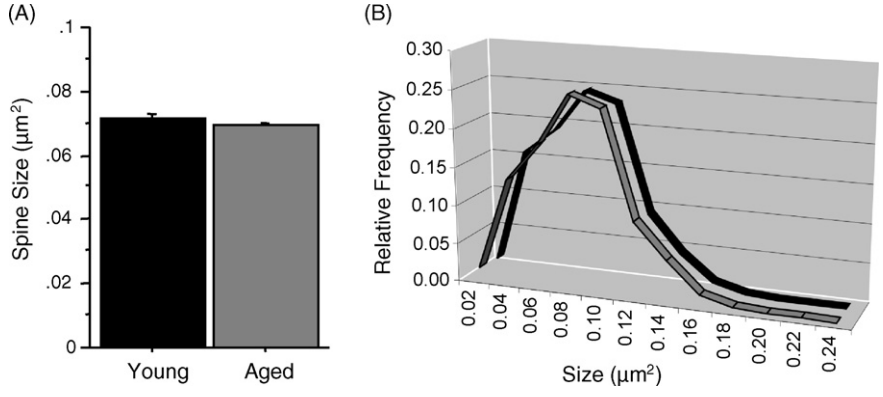

Fig. 4. Average spine size in CA1-sr. (A) No difference that could explain the observed increase in spine number was observed, and the frequency distribution of sizes (B) was also equivalent with age.

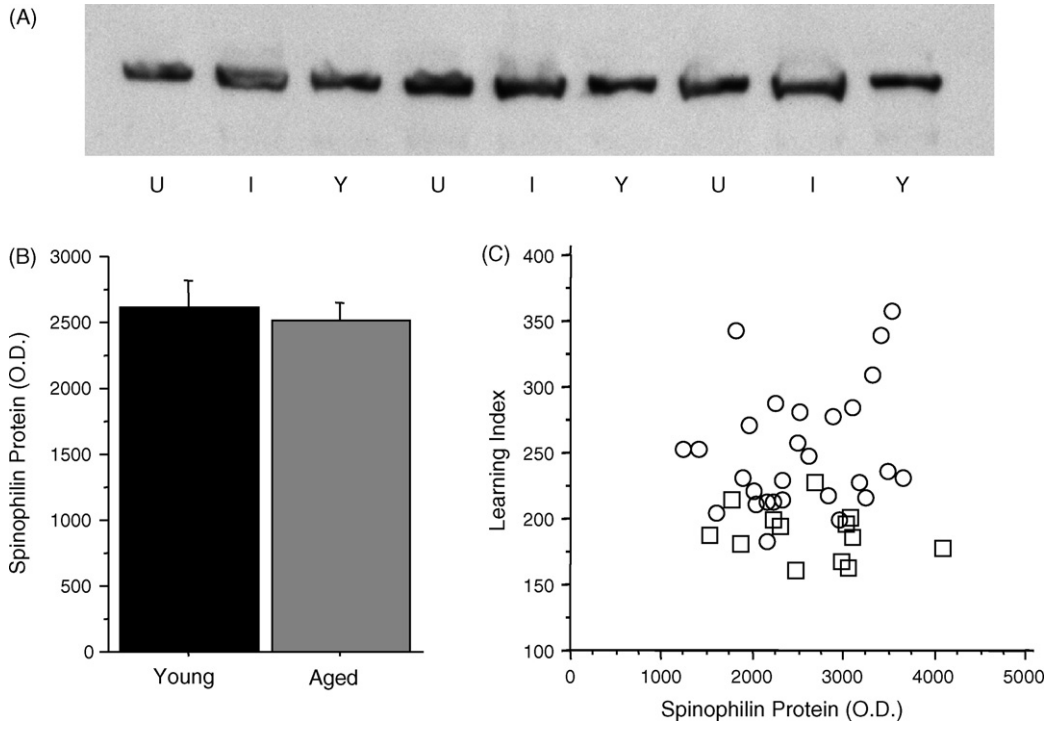

Fig. 5. Spinophilin protein levels do not differ as a function of age or cognitive status. (A) A representative Western blot illustrating equivalent protein levels for the aged-unimpaired (U), aged-impaired (I) and young (Y) rats. Graphs represent spinophilin protein levels in relation to age (B) and cognitive status (C; squares: young; circles: aged).

this parameter in relation to chronological age and cognitive status.

Previous studies establish a precedent for the observation that normal aging is accompanied by regionally specific dendritic expansion (reviewed in Coleman and Flood, 1987). Across a series of investigations in humans, Coleman and colleagues reported that, whereas the dendritic extent of hippocampal CA3 pyramidal cells remains relatively stable (Flood et al., 1987a,b), neurons in other medial temporal lobe regions, including the dentate gyrus (Flood et al., 1987a,b) and parahippocampal gyrus (Buell and Coleman, 1979), exhibit a significant increase in dendritic length during normal aging, followed by regression in the "oldest old" (over 90 years), and in patients with Alzheimer's disease. This research involved the analysis of histological material stained by the Golgi–Cox method, and a potential concern is that aging influences the sensitivity or other characteristics of dendritic labeling visualized by this approach. In a more recent study in rats, however, CA1 neurons were intracellularly filled with biotin, and dendritic extent and complexity were quantified by three-dimensional computer reconstruction (Pyapali and Turner, 1996). This analysis revealed a reliable age-related increase in dendritic length, but no relationship between this morphometric effect and spatial memory as assessed by performance in the water maze. The pattern of results reported here is broadly similar, confirming by an independent approach that normal aging is associated with regionally selective dendritic spine proliferation in the hippocampus, and that this effect is unrelated to individual variability in cognitive capacities supported by the hippocampal formation.

Quantification of spinophilin immunreactive puncta number was used in the present study primarily as a window on the baseline structural status of the aged hippocampus. Increasing evidence, however, suggests that this protein contributes to the capacity for dynamic plasticity that critically supports learning and memory. The binding partner of spinophilin, PP-1, is necessary for long-term depression (LTD) (Morishita et al., 2001), and both the phosphorylation and localization of spinophilin is dependent on NMDA (Uematsu et al., 2005) and adrenergic receptor activity (Brady et al., 2005). A recent report using rats from the same study population as the present experiment demonstrated a decrease in NMDAr-dependent hippocampal (LTD) related to chronological age, along with a corresponding increase in non-NMDAr-dependent LTD in aged rats with intact spatial memory (Lee et al., 2005). Related morphological data document that age-related memory impairment in this model is correlated with the size of the post-synaptic density among perforated synapses in the CA1 field of the hippocampus (Nicholson et al., 2004). Defining the role of spinophilin in this balance of regressive and potentially compensatory events is an important topic for further investigation. Current evidence indicates that progress is likely to require multidimensional approaches, involving coordinated structural and biochemical analyses that can be related to the regulation

of dynamic synaptic events necessary for normal cognitive function.

Disclosure statement

The authors certify that they have no actual or potential conflicts of interest.

Acknowledgements

The authors would like to thank Bill Janssen and Dr. John Morrison for immuno-electron microscopy expertise; Drs. Paul Greengard and Patrick Allen for providing the spinophilin antibody. This work was supported in part by National Institutes of Health grants AG 05868 and AG 09973.

References

Allen, P.B., Ouimet, C.C., Greengard, P., 1997. Spinophilin, a novel protein phosphatase 1 binding protein localized to dendritic spines. Proc. Natl. Acad. Sci. U.S.A. 94 (18), 9956–9961.

Bodles, A.M., Barger, S.W., 2004. Cytokines and the aging brain—what we don't know might help us. Trends Neurosci. 27 (10), 621–626.

Boncristiano, S., Calhoun, M.E., Howard, V., Bondolfi, L., Kaeser, S.A., Wiederhold, K.H., Staufenbiel, M., Jucker, M., 2005. No neocortical synaptic bouton loss despite robust amyloid deposition in APP23 transgenic mice. Neurobiol. Aging 26 (5), 607–613.

Brady, A.E., Wang, Q., Allen, P.B., Rizzo, M., Greengard, P., Limbird, L.E., 2005. Alpha 2-adrenergic agonist enrichment of spinophilin at the cell surface involves beta gamma subunits of Gi proteins and is preferentially induced by the alpha 2A-subtype. Mol. Pharmacol. 67 (5), 1690–1696.

Brady, A.E., Wang, Q., Colbran, R.J., Allen, P.B., Greengard, P., Limbird, L.E., 2003. Spinophilin stabilizes cell surface expression of alpha 2B-adrenergic receptors. J. Biol. Chem. 278 (34), 32405–32412.

Brake, W.G., Alves, S.E., Dunlop, J.C., Lee, S.J., Bulloch, K., Allen, P.B., Greengard, P., McEwen, B.S., 2001. Novel target sites for estrogen action in the dorsal hippocampus: an examination of synaptic proteins. Endocrinology 142 (3), 1284–1289.

Buell, S.J., Coleman, P.D., 1979. Dendritic growth in the aged human brain and failure of growth in senile dementia. Science 206 (4420), 854–856.

Calhoun, M.E., Jucker, M., Martin, L.J., Thinakaran, G., Price, D.L., Mouton, P.R., 1996. Comparative evaluation of synaptophysin-based methods for quantification of synapses. J. Neurocytol. 25 (12), 821–828.

Calhoun, M.E., Kurth, D., Phinney, A.L., Long, J.M., Hengemihle, J., Mouton, P.R., Ingram, D.K., Jucker, M., 1998. Hippocampal neuron and synaptophysin-positive bouton number in aging C57BL/6 mice. Neurobiol. Aging 19 (6), 599–606.

Coleman, P.D., Flood, D.G., 1987. Neuron numbers and dendritic extent in normal aging and Alzheimer's disease. Neurobiol. Aging 8 (6), 521–545.

Flood, D.G., Buell, S.J., Horwitz, G.J., Coleman, P.D., 1987a. Dendritic extent in human dentate gyrus granule cells in normal aging and senile dementia. Brain Res. 402 (2), 205–216.

Flood, D.G., Guarnaccia, M., Coleman, P.D., 1987b. Dendritic extent in human CA2-3 hippocampal pyramidal neurons in normal aging and senile dementia. Brain Res. 409 (1), 88–96.

Futter, M., Uematsu, K., Bullock, S.A., Kim, Y., Hemmings Jr., H.C., Nishi, A., Greengard, P., Nairn, A.C., 2005. Phosphorylation of spinophilin by ERK and cyclin-dependent PK 5 (Cdk5). Proc. Natl. Acad. Sci. U. S. A. 102 (9), 3489–3494.

Gallagher, M., Bizon, J.L., Hoyt, E.C., Helm, K.A., Lund, P.K., 2003. Effects of aging on the hippocampal formation in a naturally occurring animal model of mild cognitive impairment. Exp. Gerontol. 38 (1–2), 71–77.

Gallagher, M., Burwell, R., Burchinal, M., 1993. Severity of spatial learning impairment in aging: development of a learning index for performance in the Morris water maze. Behav. Neurosci. 107 (4), 618–626.

Gallagher, M., Rapp, P.R., 1997. The use of animal models to study the effects of aging on cognition. Annu. Rev. Psychol. 48, 339–370.

Geinisman, Y., Ganeshina, O., Yoshida, R., Berry, R.W., Disterhoft, J.F., Gallagher, M., 2004. Aging, spatial learning, and total synapse number in the rat CA1 stratum radiatum. Neurobiol. Aging 25 (3), 407–416.

Halpain, S., Spencer, K., Graber, S., 2005. Dynamics and pathology of dendritic spines. Prog. Brain Res. 147, 29–37.

Hao, J., Janssen, W.G., Tang, Y., Roberts, J.A., McKay, H., Lasley, B., Allen, P.B., Greengard, P., Rapp, P.R., Kordower, J.H., Hof, P.R., Morrison, J.H., 2003. Estrogen increases the number of spinophilin-immunoreactive spines in the hippocampus of young and aged female rhesus monkeys. J. Comp. Neurol. 465 (4), 540–550.

Hof, P.R., Morrison, J.H., 2004. The aging brain: morphomolecular senescence of cortical circuits. Trends Neurosci. 27 (10), 607–613.

Lee, H.K., Min, S.S., Gallagher, M., Kirkwood, A., 2005. NMDA receptor-independent long-term depression correlates with successful aging in rats. Nat. Neurosci. 8 (12), 1657–1659.

Morishita, W., Connor, J.H., Xia, H., Quinlan, E.M., Shenolikar, S., Malenka, R.C., 2001. Regulation of synaptic strength by protein phosphatase 1. Neuron 32 (6), 1133–1148.

Nicholson, D.A., Yoshida, R., Berry, R.W., Gallagher, M., Geinisman, Y., 2004. Reduction in size of perforated postsynaptic densities in hippocampal axospinous synapses and age-related spatial learning impairments. J. Neurosci. 24 (35), 7648–7653.

Nicolle, M.M., Gallagher, M., McKinney, M., 1999. No loss of synaptic proteins in the hippocampus of aged, behaviorally impaired rats. Neurobiol. Aging 20 (3), 343–348.

Ouimet, C.C., Katona, I., Allen, P., Freund, T.F., Greengard, P., 2004. Cellular and subcellular distribution of spinophilin, a PP1 regulatory protein that bundles F-actin in dendritic spines. J. Comp. Neurol. 479 (4), 374–388.

Pyapali, G.K., Turner, D.A., 1996. Increased dendritic extent in hippocampal CA1 neurons from aged F344 rats. Neurobiol. Aging 17 (4), 601–611.

Radley, J.J., Rocher, A.B., Miller, M., Janssen, W.G., Liston, C., Hof, P.R., McEwen, B.S., Morrison, J.H., 2005. Repeated stress induces dendritic spine loss in the rat medial prefrontal cortex. Cereb. Cortex 16 (3), 313–320.

Rapp, P.R., Gallagher, M., 1996. Preserved neuron number in the hippocampus of aged rats with spatial learning deficits. Proc. Natl. Acad. Sci. U. S. A. 93 (18), 9926–9930.

Rasmussen, T., Schliemann, T., Sorensen, J.C., Zimmer, J., West, M.J., 1996. Memory impaired aged rats: no loss of principal hippocampal and subicular neurons. Neurobiol. Aging 17 (1), 143–147.

Rosenzweig, E.S., Barnes, C.A., 2003. Impact of aging on hippocampal function: plasticity, network dynamics, and cognition. Prog. Neurobiol. 69 (3), 143–179.

Satoh, A., Nakanishi, H., Obaishi, H., Wada, M., Takahashi, K., Satoh, K., Hirao, K., Nishioka, H., Hata, Y., Mizoguchi, A., Takai, Y., 1998. Neurabin-II/spinophilin. An actin filament-binding protein with one pdz domain localized at cadherin-based cell-cell adhesion sites. J. Biol. Chem. 273 (6), 3470–3475.

Smith, T.D., Adams, M.M., Gallagher, M., Morrison, J.H., Rapp, P.R., 2000. Circuit-specific alterations in hippocampal synaptophysin immunoreactivity predict spatial learning impairment in aged rats. J. Neurosci. 20 (17), 6587–6593.

Tang, Y., Janssen, W.G., Hao, J., Roberts, J.A., McKay, H., Lasley, B., Allen, P.B., Greengard, P., Rapp, P.R., Kordower, J.H., Hof, P.R., Morrison, J.H., 2004. Estrogen replacement increases spinophilin-immunoreactive spine number in the prefrontal cortex of female rhesus monkeys. Cereb. Cortex 14 (2), 215–223.

Terry-Lorenzo, R.T., Roadcap, D.W., Otsuka, T., Blanpied, T.A., Zamorano, P.L., Garner, C.C., Shenolikar, S., Ehlers, M.D., 2005. Neurabin/protein phosphatase-1 complex regulates dendritic spine morphogenesis and maturation. Mol. Biol. Cell 16 (5), 2349–2362.

Uematsu, K., Futter, M., Hsieh-Wilson, L.C., Higashi, H., Maeda, H., Nairn, A.C., Greengard, P., Nishi, A., 2005. Regulation of spinophilin Ser94 phosphorylation in neostriatal neurons involves both DARPP-32-dependent and independent pathways. J. Neurochem. 95 (6), 1642–1652.

Wang, X., Zeng, W., Soyombo, A.A., Tang, W., Ross, E.M., Barnes, A.P., Milgram, S.L., Penninger, J.M., Allen, P.B., Greengard, P., Muallem, S., 2005. Spinophilin regulates Ca2+ signalling by binding the N-terminal domain of RGS2 and the third intracellular loop of G-protein-coupled receptors. Nat. Cell Biol. 7 (4), 405–411.

West, M.J., Slomianka, L., Gundersen, H.J., 1991. Unbiased stereological estimation of the total number of neurons in the subdivisions of the rat hippocampus using the optical fractionator. Anat. Rec. 231 (4), 482–497.